Changes in the Tertiary Structure of α-Chymotrypsin with Change in pH; pH 4.2–6.7†

Richard L. Vandlen‡ and Alexander Tulinsky*

ABSTRACT: The pH of single crystals of α-chymotrypsin has been changed from 4.2 to 6.7 with a concomitant change in the intensities of the X-ray diffraction pattern. The three-dimensional changes of the pattern at 2.8-Å resolution have been related to changes in the tertiary structures of the two independent molecules of α-chymotrypsin in the asymmetric unit. The majority of the differences observed with increase in pH are located primarily on the surfaces of the enzyme molecules or in the interface regions between two molecules comprising a dimeric structure. The differences are generally associated with amino acid residues with polar side chains. The largest differences occur with the carboxylic acid groups of the two B-chain terminal Tyr-146 residues which enter into an important dimer interface interaction with bridging sulfate ions that hydrogen bond to the hydroxyl of Tyr-146 of one molecule and the hydroxyl of the catalytically important Ser-195 of the other molecule. Changes also occur at other dimer interface interactions, Ala′-149$^+$ and Asp-64$^-$, Phe-39 and its local twofold counterpart Phe′-39, Ser-217–Ser-218 and Met-192. The region near His-40 shows large changes in the orientation of the imidazole ring and large changes are also observed near a unique intermolecular interaction site. The foregoing changes have been related to the behavior of dimerization equilibrium constants with pH (interface), fluorescence quenching with decreasing pH (His-40) and specific site–site charge configuration interactions (intermolecular Glu-21–Asp′-153). The structure of the interior of the molecule remains essentially unaltered with an increase in pH.

Chemical, physical, and biochemical studies of biological macromolecules such as proteins can be used to obtain information concerning the effects of pH, solvent changes, and other environmental variables on the structure and reactivity of these molecules in solution. Detailed interpretation of the results depends to a large degree on the knowledge of the three-dimensional structure of the molecule as determined by X-ray crystallographic methods. The relatively large interstitial spaces between molecules in protein crystals and the large porportion of solvent occupying them basically permit the molecules to retain a conformation in the crystal similar to that in solution, even though the molecule is constrained in an ordered matrix. The assumption that the structure of a globular protein in the crystal is approximately the same as the structure in solution has been tested in a variety of ways and has been found to be generally valid (Doscher and Richards, 1963; Quiocho and Richards, 1966; Rossi and Bernhard, 1970). Likewise, X-ray crystallographic observations of movements of protein chains or amino acid residues within a molecule after interaction or reaction with substrate-like or inhibitor molecules have been taken to be important observations which relate to the manner in which the molecule functions. While the effects of various substrate or inhibitor molecules on protein crystals structures have been widely investigated for a number of proteins, little attention has heretofore been given to the effect on such structures of pH, salt composition, and other variables which deal with the aqueous medium surrounding the molecules. It is with such effects that we have concerned ourselves in this work.

The hydrogen ion concentration of the aqueous medium plays an important role in the structure–function relationships of all biological macromolecules. At extremes of pH, most protein molecules denature, while near physiological pH values they display their optimal activity. Since proteins contain a number of amino acid residues whose side chains can ionize in the pH range of 2–13, and since it has been shown that a large amount of conformational stability can be conferred on a macromolecule by appropriate interactions between these particular amino acid residues either through ionic interactions or by hydrogen bonding, it is clear that the conformation of biological macromolecules is intimately dependent on the hydrogen ion concentration of the surrounding medium.

The effect of the hydrogen ion concentration of the aqueous medium on the conformation and activity of α-chymotrypsin is manifested in several different ways. The activity of α-chymotrypsin has been shown to be pH dependent and is affected by the ionization states of several amino acids in and around the active site of the molecule (Bender *et al.*, 1964; Hess, 1971). A number of different thermodynamic states representing various stages of folding or unfolding of the peptide chains are also accessible by changes in pH (Lumry and Biltonen, 1969). Furthermore, the association of α-chymotrypsin into dimeric molecules has been shown to be dependent upon pH and other solvent parameters (Schwert, 1949; Schwert and Kaufman, 1951; Aune and Timasheff, 1971; Aune *et al.*, 1971). The three-dimensional structure of the dimeric native state of α-chymotrypsin has been determined by us (Tulinsky *et al.*, 1973a,b) and the structure of a dimeric inhibited form of the molecule, tosyl-α-chymotrypsin (toluenesulfonyl), has been determined by Blow and his coworkers (Matthews *et al.*, 1967; Birktoft and Blow, 1972). In both cases, the structures were solved at a pH of ~4.0, the pH at which well-formed crystals can be grown easily. Since optimal catalytic activity of α-chymotrypsin is in the neighborhood of pH ~8.0, it seemed desirable to investigate

† From the Departments of Chemistry and Biochemistry, Michigan State University, East Lansing, Michigan 48824. *Received April 2, 1973.* This work was supported by the National Science Foundation, Molecular Biology Section, Grants GB-6586, GB-7399, and GB-15402.

‡ Present address: Chemistry Division, California Institute of Technology, Pasadena, Calif. 91109.

TABLE 1: Unit Cell Dimensions of α-Chymotrypsin Crystals at pH 6.7 and 4.2.

	pH 6.7	Native
a	49.13 (5) Å	49.24 (7) Å
b	67.83 (7) Å	67.20 (10) Å
c	65.81 (7) Å	65.94 (9) Å
β	101.92 (6)°	101.79 (6)°
Cell volume	214,500 ± 700 Å^3	213,400 ± 900 Å^3

the structure at higher pH values in order to determine whether conformational changes accompany change in pH. We have already reported that the structure in the crystalline state is different at pH 6.7 than that observed at pH 4.2 (Vandlen and Tulinsky, 1971a). We now wish to detail the observed effects on the tertiary structure of α-chymotrypsin at 2.8 Å resolution which occur on changing the pH from 4.2 to 6.7.

Experimental Section

Worthington Biochemical Corp. α-chymotrypsin, three times crystallized, was used in all the work without further purification. The crystals employed in the X-ray crystallographic studies were grown from about 50% saturated ammonium sulfate solutions at pH 4.2 and they were stored in 75% saturated ammonium sulfate at the same pH. The hydrogen ion concentration of the ammonium sulfate soaking solution of the crystals was changed from pH 4.2 to 7.5 and higher *via* slow addition of ammonium hydroxide. Sudden pH changes resulted in most of the crystals becoming severely cracked; slower changes of pH, usually over a 2-week period, produced less severely cracked crystals with some crystals having no observable cracks. Uncracked crystals were used in all the X-ray diffraction experiments even though the diffraction pattern of less severely cracked crystals was the same as the former.

The X-ray diffraction patterns along the principal axial directions were recorded for a series of crystals as a function of pH during the time interval required to change the pH from 4.2 to about 7.5. Differences in the intensities among the diffraction patterns of crystals with pH between 4.2 and 5.0 were negligible, although the *b* axis became progressively larger as the pH was increased (from 67.2 to about 68.0 Å). Over a fairly narrow range of pH between 5.0 and 5.6, the crystals generally became cracked and this was accompanied by substantial changes in the intensities of the diffraction pattern. From pH ~6.0 to 8.0 only minor additional changes in the pattern were observed; however, above pH 8.0, another fairly sharp onset of intensity changes occurred. The foregoing changes are apparently also reversible since the higher pH axial diffraction patterns revert to that of pH 4.2 on lowering the pH of the soaking solution. Crystals at pH 6.7, intermediate between the two transition pH values, were initially chosen for three-dimensional structural studies. Other studies are in progress on crystals with pH values of 8.6 and less than 4.2.

The stability and quality of the diffraction pattern of crystals at pH 6.7 were comparable to that of the native enzyme crystals at pH 4.2.[1] Moreover, the diffraction pattern of the higher pH crystals from several different crystallization batches showed excellent reproducibility. The average unit cell dimensions measured from four different crystals at pH 6.7 are compared to the cell dimensions of the native enzyme in Table I. The observed standard error of each dimension is given in parentheses. The *a* and *c* axes are approximately the same length at the two pH values, while the length of the *b* axis increases significantly by about 0.6 Å upon change of pH and causes a slight net increase in the volume of the unit cell (0.5%). The interaxial angle remains essentially unaltered with an increase in pH.

The three-dimensional intensity data at 2.8 Å resolution of the pH 6.7 crystals were collected in a manner similar to that described elsewhere (Vandlen and Tulinsky, 1971b; Tulinsky *et al.*, 1973a) with a Picker four-circle automatic diffractometer controlled by a Digital Equipment Corporation PDP-8 computer coupled to a DEC 32K disc file and an Ampex TMZ 7-track tape transport. In order to confine the intensity data collection to a minimum number of crystals, only those reflections which had a figure of merit, *m* (Blow and Crick, 1959), greater than 0.7 were measured. These corresponded to the reflections for which the native enzyme phases were most reliably determined by the use of the multiple isomorphous replacement method with six heavy atom isomorphous derivatives (Tulinsky *et al.*, 1973a). In this manner, only about 6300 reflections had to be considered to 2.8-Å resolution and they were measured from one crystal within 4 days time. X-Ray damage to the crystal was minimized by operating the X-ray tube at about 500 W. Monitored reflections with high 2θ values were measured periodically every hour during the data collection and they showed a total decrease of approximately 30% from their initial intensities after 73 hr of X-ray exposure. Since the effect of X-ray damage is a function of 2θ and it is most pronounced at higher Bragg angles, the 2500 reflections with spacings from 3.5 to 2.8 Å were measured first and they suffered a maximum decrease in intensity of less than 10%. The lower resolution data collection followed with the overall decay in this range being substantially less than the 30% total decrease recorded for the monitored reflections (about 15%). Thus the decays of the intensities of the two ranges were comparable.

The measured intensities were placed on an approximate absolute scale and were corrected for absorption, twin size, and decay factors in a manner described elsewhere (Tulinsky *et al.*, 1973a) before conversion to structure amplitudes. The approximate scale of the resultant structure amplitudes was given a final adjustment by fitting the radial $|F|^2$ distribution curve of the pH 6.7 amplitudes to that of the native data at higher Bragg angles.

A "best" difference electron density map between the structure of α-chymotrypsin at pH 6.7 and that at pH 4.2 was computed using coefficients of the form

$$m(|F_{PH}| - |F_P|) \exp(i\alpha_P)$$

where $|F_{PH}|$ and $|F_P|$ are the structure amplitudes at pH 6.7 and the native enzyme, respectively, *m* is the figure of merit of a reflection, and α_P is the "best" phase angle at pH 4.2 (Blow and Crick, 1959). The difference electron density was computed in the same way as the native electron density map (scale, grid intervals, etc.) and it was contoured onto the Plexiglass sheets of the native enzyme density. With the aid of an optical comparator (Richards, 1968), the structural changes which accompany the change in pH were then related

[1] The structure of native α-chymotrypsin at pH 4.2 will hereafter be referred to as the native structure or the pH 4.2 structure while that of the native enzyme at pH 6.7 will simply be referred to as the pH 6.7 structure.

directly to the Kendrew models of the *two independent molecules* of α-chymotrypsin in the asymmetric unit of the crystal.

Results

General. The difference electron density map between the structure of α-chymotrypsin at pH 6.7 and at pH 4.2 revealed a relatively broad distribution of a large number of positive and negative regions substantially above or below the average background of the difference map. These regions proved to represent differences in tertiary structure at the two different pH values. The majority of the differences were small and observed to be located primarily on the surfaces of the enzyme molecules or in an interface region between the two molecules of the asymmetric unit; few differences were observed in the nonpolar interior of the molecule. The differences were generally associated with amino acid residues with polar side chains and the solvent-containing regions between adjacent molecules in the crystal were essentially devoid of any significant peaks in the difference electron density.

At a number of places in the difference electron density map a positive region is accompanied by a negative region of approximately the same magnitude located on either side of a peak in the native electron density. These electron density gradients indicate a movement of *a group of atoms or residue* of the original electron density. The magnitude of the positional shift from r_1 to r_2 can be estimated approximately from the slope of the difference electron density and the curvature of the corresponding electron density at the original position, r_1

$$\Delta r = (r_2 - r_1) = -\text{slope/curvature}$$

$$\Delta r = -(\partial \Delta\rho/\partial r)_{r_1}/(\partial^2\rho/\partial r^2)_{r_1}$$

where $\Delta\rho$ is the difference electron density and the partial derivatives are evaluated at $r = r_1$. The largest peaks in the difference electron density were approximately ±(0.3–0.4 eÅ^{-3}). The largest difference density gradients were about 0.4 eÅ^{-4} while the curvatures in the electron density were of the order of 0.7–0.9 eÅ^{-5}. The positional shifts *of groups of atoms* which correspond to these values are about 0.3–0.5 Å. However, since the difference electron density is truly given by coefficients of the form

$$|F|_{PH} \exp(i\alpha_{PH}) - |F|_{P} \exp(i\alpha_{P})$$

where α_{PH} is the phase angle at pH 6.7, the peak heights of the difference density reported above are generally smaller by up to a factor of two (Luzzatti, 1953), so that the positional shifts are also correspondingly larger by this amount (up to ~1.0 Å). The root-mean-square error of the difference density was computed to be about ±0.02 eÅ^{-3} (Henderson and Moffat, 1971), but the average value of the largest noise peaks of the difference map was typically ±0.05 eÅ^{-3}. Thus, the largest observed differences were six–eight times the latter density and even larger when exact phasing is considered.

The crystallographic asymmetric unit of α-chymotrypsin consists of two independent molecules related to one another by a noncrystallographic or local twofold rotation axis (Blow *et al.*, 1964; Cohen *et al.*, 1970; Tulinsky *et al.*, 1973a). A schematic packing diagram of α-chymotrypsin in the unit cell is shown in Figure 1, which also shows, in part, the shape of a molecule. The shape approximates a prolate ellipsoid

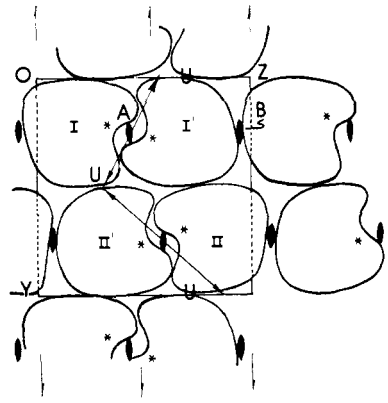

FIGURE 1: Schematic packing diagram of α-chymotrypsin viewed along the a^* direction. Molecules I and I′ form an asymmetric unit and are related by noncrystallographic twofold rotation axes A and B; asymmetric units related by crystallographic twofold screw axes parallel to y axis; active-site regions near center of dimer designated with asterisks; uranyl binding region designated by U; local twofold U′ position located at ends of arrows.

of about 25 × 28 × 33 Å with a section missing consisting of about one-eighth of its surface along the major axis; this depression penetrates about 10 Å deep into the molecule and the active site is located off the center of this elongated basin. Molecules I and I′ of Figure 1 form an asymmetric unit and are related to one another by the local twofold axis designated A. Molecules II and II′ belong to the second asymmetric unit of the crystal and are related to the first by the crystallographic twofold screw axes appropriately shown in Figure 1. Molecules I and I′ are fairly complementary to one another around dyad A and form a relatively large number of intimate polar and nonpolar interactions whereas few interactions occur around dyad B. The region around dyad A will hereafter be referred to as the dimer interface region. The major interactions between the two molecules at pH 4.2 in the dimer interface are given in Figure 2, where the local dyad A is depicted as the horizontal line. The amino acid residues with the prime notation belong to molecule I′ in the asymmetric unit. All subsequent references to this molecule will use that notation. The main ionic interactions between the two molecules are: the carboxylate group of Asp-64 and the amino terminal of the C chain, Ala′-149 (Asp-35 is also in the vicinity), and, possibly, the terminal carboxylate group of the B chain, Tyr′-146, and the imidazolium ion of His-57.[2] These groups are all presumably charged at pH 4.2. The electron density in the vicinity of Ala-149 is not as well defined as its local twofold counterpart so that the corresponding twofold interaction is uncertain to this extent. Additional interactions across the twofold axis involve the side chains of Met-192 and Met′-192, the main chains of residues Ser-217–Ser-218 and Ser′-217–Ser′-218, and the side chains of Phe-39 and Phe′-39 (Tulinsky *et al.*, 1973b).

From ammonium sulfate–ammonium selenate exchange experiments (Tulinsky and Wright, 1973), an important dimer interface interaction was established in which a sulfate ion forms a bridge between the two molecules of the asymmetric unit through hydrogen bonding between the hydroxyl group of Tyr-146 of one molecule and the hydroxyl group of Ser-195 of the other molecule of the asymmetric unit (Figures 2 and 3). The corresponding twofold interaction involving an-

[2] A plausible alternative for the latter is a hydrogen-bond interaction between an un-ionized carboxyl group of Tyr′-146 and the carbonyl of His-57. This possibility will be discussed later.

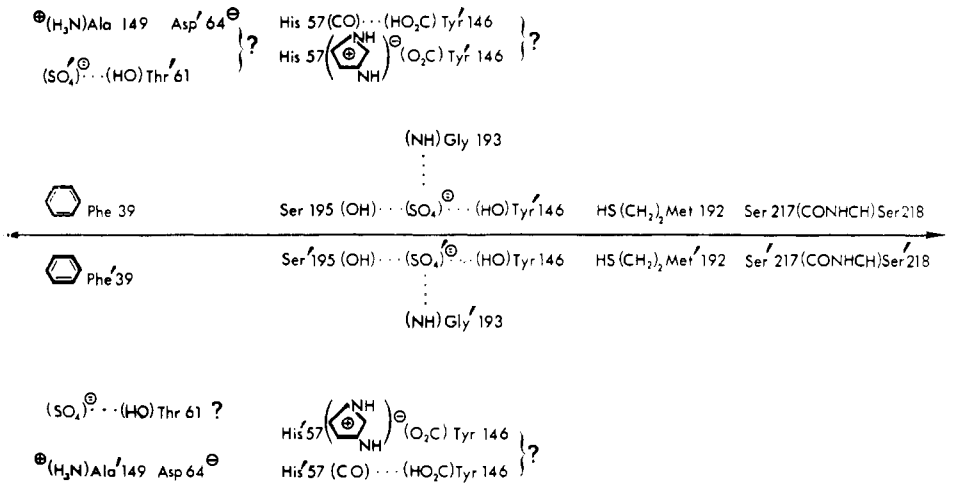

FIGURE 2: Dimer interface region of α-chymotrypsin at pH 4.2 showing intermolecular interactions and close contacts across dyad A; molecule I, unprimed; molecule I′, primed.

other sulfate ion, Tyr-146, and Ser-195 is also operative. In addition, there are other localized sulfate ions in the crystal structure, such as the one indicated in Figure 2 which participates in a complicated interaction involving Thr′-61, Asp′-64, Ala-149, and possibly Asp′-35. The corresponding twofold equivalent sulfate ion appears less well defined and at a lower level in the sulfate–selenate difference electron density maps; in addition, the two sulfates deviate about 3.0 Å from local twofold symmetry suggesting that the equivalent intermolecular interactions in this vicinity might be different.

Dimer Interface Region. The largest change is associated with the carboxylic acid groups of the B-chain terminal residues of Tyr-146 and Tyr′-146. The difference electron density possesses large positive peaks of about 0.35 eÅ^{-3} near the position of the carboxyl groups of both Tyr residues with an accompanying negative peak of the same height positioned at the electron density assigned to one of the oxygen atoms of the carboxyl group in the pH 4.2 structure. The electron density map in the vicinity of Tyr′-146 and His-57 is shown in Figure 4 with the ΔpH difference map superimposed in white contours. The arrangement of residues in the vicinity of this interaction is shown in Figure 3. At pH 4.2, the imidazole of His-57 is protonated and the charge of the imidazolium ion of one molecule can interact with the carboxylate ion to Tyr′-146 of the other molecule and the bridging sulfate ion, with a corresponding interaction between His′-57, Tyr-146, and another bridging sulfate ion; alternatively, the carboxyl group of Tyr′-146 might not be ionized and the hydroxyl group (atom O_2) forms a hydrogen bond with the carbonyl of His-57. Although this alternative will be discussed in more detail below, we will continue to refer to the carboxylic acid group as the carboxylate ion.

The net result implied by the difference and electron density maps is a movement of the carboxylate group from its position in the native enzyme to one such that O_1 occupies a position near that formally occupied by O_2, and O_2 moves to a new position at the positive electron density of the difference map. This is apparently accomplished by a 40–50° clockwise rotation of the carboxylate group around the C_α atom of Tyr′-146 and a small counterclockwise rotation of the C_α around the NH–C_α bond.[3] Since the hydrogen-bonding network among the hydroxyl group of Tyr′-146, the bridging sulfate ion, and the hydroxyl of Ser-195 *is not affected by the change in pH*, the phenolic end of Tyr′-146 remains essentially fixed and the above rotations effectively correspond to a linear displacement of the carboxylate group of about 1.0 Å parallel to the local twofold axis toward the phenyl ring. Moreover, the plane of the imidazole of His-57 shifts slightly toward Tyr′-146. This is accomplished by a small clockwise rotation of C_β and thus the imidazole ring around the C_α–C_β bond. A similar overall movement is observed with the local twofold related carboxylate group of Tyr-146.

Other changes occur in the dimer interface around the ionic interaction between the nitrogen of the N-terminal amino group of Ala′-149 of one molecule (C chain) and the side-chain carboxylate ion of Asp-64 of the twofold related molecule. As previously mentioned, the residues of Ala′-149 and Asp-64 are well defined in the electron density but the twofold related pair is not nearly as clear. This is probably because the latter residues are involved in an even more complicated arrangement and interaction which additionally involves the side chains of Asp′-35, Asp-153, Lys′-36, and a localized sulfate ion. The latter forms a hydrogen bond with the hydroxyl group of Thr′-61. At the higher pH, a negative peak in the difference map coincides with the electron density of the sulfate ion and suggests the loss or movement of the sulfate ion from its original position. A detailed interpretation of the observed changes in this region is difficult, but nevertheless, it is clear that substantial protein rearrangements take place at this interaction site upon change of pH.

Upon examination of some of the nonionic interactions which occur in the interface region (Figure 2), it becomes obvious that the general disruption and weakening of the ionic interactions which accompanies change in pH also disturb other interactions as well.[4] Two sets of van der Waals interactions (Phe-39, Phe′-39 and Ser-217–Ser-218,Ser′-217–

[3] When a rotation around a bond is discussed, the bond is taken as the rotation axis and the sense of the axis is taken from the first to the second atom of the bond.

[4] There are four other close-contact pairs which might be involved in a dimer interface interaction: Lys′-36$^+$–Asp-153$^-$; Thr′-151(NH)···(O_2C)Asp-35; Arg′-145(NH)···(HO)Ser-96; and Asn-148(NH_2)···(OC)Gly′-59. These interactions are less definitive because they do not possess a local twofold counterpart and because the contact distances in the latter three are borderline for a hydrogen-bonding interaction; with Lys′-36, the density is ill-defined beyond C_γ. The correct status of the interactions should be fixed during the course of the refinement of the structure.

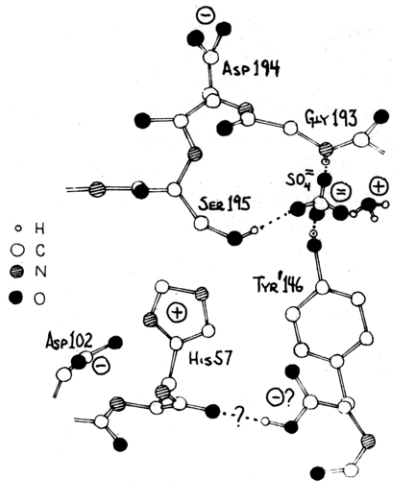

FIGURE 3: Drawing of α-chymotrypsin model at pH 4.2 in vicinity of active site viewed down local twofold axis. Dyad A designated by dyad symbol; bridging sulfate and counterion shown; hydrogen bonds depicted by broken lines.

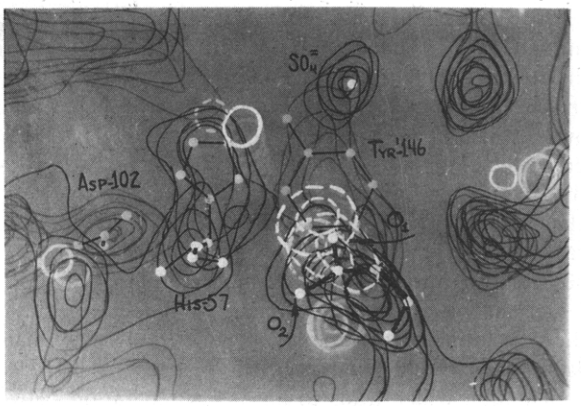

FIGURE 4: Electron density near His-57–Tyr′-146 of α-chymotrypsin at pH 4.2. Contours at 0.25 eÅ^{-3} (1.4σ), beginning with 0.5 eÅ^{-3} (2.8σ); difference electron density between pH 6.7 and 4.2 shown in white; contours at 0.15 eÅ^{-3} (6σ), beginning with 0.15 eÅ^{-3}; solid contours, positive; broken contours, negative; positions of His-57, Asp-102, and Tyr′-146 shown; O_1 and O_2 are carboxylate oxygen atoms of Tyr′-146; bridging sulfate ion designated SO_4^{2-}

Ser′-218), which must undergo some initial mutual accommodation at the time of the formation of a dimeric species (Tulinsky *et al.*, 1973b), show changes in the difference electron density. The two Phe-39 residues are situated so that their phenyl rings are practically in contact with the local twofold axis of the interface region. The ΔpH difference density in this region implies differing motions for the two residues. The carboxyamide of the main chain between Gly-38 and Phe-39 pivots about the C_α atoms of Thr-37 and Phe-39 and moves 0.7 Å or so toward the side chain of Gln-34, or in a general direction away from the local twofold axis and toward the bulk of the molecule. There is an accompanying positive difference electron density on the phenyl group of Phe-39 which might represent a small shift in position or perhaps a better ordering of the group at the higher pH (*e.g.*, higher electron density). The main chain of Phe′-39 (NH–C_α–CO) moves about the same distance along the twofold axis toward the solvent region of the crystal which begins nearby. Moreover, the foregoing movements are accomplished in a manner which maintains the close van der Waals contacts between the two nearly parallel phenyl groups observed at pH 4.2. There are also movements of the main chain of Ser-217–Ser-218 but very little change with the twofold related segment (a slight alteration appears near the amide between Gly′-216 and Ser′-217). The main chain amide between Ser-217 and Ser-218 rotates about 20–30° about the α-carbon atoms toward the interior of the molecule (along the twofold axis). This is also close to the maximum possible rotation for the amide without seriously disrupting the main chain conformation in this region and it reduces simply to a translation of the amide nitrogen and the carbonyl oxygen of about 0.6–0.7 Å. The carboxyamide was not originally coplanar with its twofold equivalent (Tulinsky *et al.*, 1973b) and the variation is magnified at pH 6.7. Small accompanying changes are also observed to occur with the respective side chains of these residues.

His-40. The His-40 residue is on the surface on a single molecule near the interface region of the dimeric molecule. However, there is no apparent interaction between the His-40 residue and its twofold related residue. The imidazole ring of His-40 is directed toward the interior of each molecule. One edge of the imidazole ring is near Ser-32 and Asp-72 and is relatively accessible to solvent, even in the dimeric molecule, while the other edge is bounded by residues Gly-193–Asp-194 and the imidazole ring resides between Cys-42–Gly-43 and Trp-141–Gly-142. The indole ring of Trp-141 is nearly parallel to the imidazole at an interplanar separation of ~4.0 Å. Moreover, the orientation of the imidazole of His-40 is somewhat different in the two independent molecules of α-chymotrypsin at pH 4.2. In molecule I′, the N_ϵ atom of His′-40 is appreciably closer to the carbonyl oxygen of the carboxyamide of Gly′-193 (~4.0 Å); in addition, the side chain of Ser-32 approaches the N_δ position within about 3.5 Å. However, Ser-32 appears to be hydrogen bonding with neighboring Asp-72. With molecule I, the imidazole is rotated clockwise about 30° around the C_α–C_β bond from this orientation and results in a position where neither of the foregoing interactions are particularly favorable.[5] The ΔpH difference map shows a large positive density overlapping the edge of the electron density corresponding to the imidazole ring with a corresponding negative peak on the opposite side of the ring. This pair of peaks implies a movement of the imidazole in the plane of its ring about 0.8 Å toward Gly-193. This is achieved by the rotation of the C_β atom of 20–30° in a counterclockwise manner about the C_α–C_β bond. A slightly different but similar net motion is observed with His′-40.

Uranyl Binding Region. In addition to the intermolecular interactions which occur in the dimer interface, there is another region in which a number of interactions are found between the independent molecules of the asymmetric unit. This region, designated by U in Figure 1, is formed by the proximity of surface contacts between molecules I and II′ in the *xz* plane of the crystal. It is also the dominant intermolecular binding site of our uranyl heavy atom isomorphous derivative (Tulinsky *et al.*, 1973a). Only one such intermolecular site exists per asymmetric unit because the enzyme environment of the local twofold counterpart region, which is generated by a twofold screw axis operation on the asymmetric unit, is not the same and consequently is incapable of binding a uranyl ion intermolecularly. The main chains of the respective residues of the independent molecules in the twofold equivalent region are basically similar and the same is

[5] If the imidazole of His-40 were rotated about its C_β–C_γ bond by 180°, then the N_ϵ atom would be in a better position to hydrogen bond with the hydroxyl of Ser-32 as a hydrogen donor. The correct alternative is not clear at this time.

true of the orientation and overall configuration of the side chains; however, the two molecules are separated by a larger translational contact in the twofold related region (6–7 Å as compared to 3–4 Å). This can be seen from Figure 1 which shows a different intermolecular contact for the twofold related uranyl binding region. The carboxylate groups of Glu-21 and Asp′-153 in this region are close enough spatially to chelate a uranyl ion; the reciprocal interaction does not occur because these groups are too far apart for the chelation interaction. The situation is further complicated in this region by the fact that certain residues possess different orientations and/or conformations in the independent molecules (blatant lack of local twofold symmetry). For instance, Asp-153 is in an orientation which leads to an 8–9 Å separation between Glu′-21 and Asp-153. The different orientation brings the carboxylate group of Asp-153 into a position such that it might enter into an ionic dimer interface interaction with the ϵ-amino nitrogen atom of the Lys′-36 side chain. However, the interaction is somewhat ambiguous because the Lys side chain is not well defined beyond C_γ.

The structural changes of the two molecules in this region are very complicated when the pH of the soaking solution is raised to 6.7. An apparent complex between a localized sulfate ion and the guanidinium group of Arg-154 is disrupted when the latter moves toward Glu-21; moreover, the carboxylate group of Glu-21 reciprocates by pivoting about its C_α or C_β atom toward Arg-154. In addition, there are a number of other changes which are apparently associated with localized solvent molecules that are present in this region in the native electron density map. All these movements combine to considerably alter the environment around this unique intermolecular contact region. In complete contrast, the corresponding twofold equivalent region shows no ΔpH induced changes.

Discussion

Dimer Interface Region. The large number of ΔpH difference electron density peaks which are concentrated in the interface region of the dimeric molecule are undoubtedly related to the initial structural changes which take place upon the dissociation of dimeric molecules with increasing pH. The sedimentation constant of α-chymotrypsin is pH dependent and has a maximum near pH 4.0 (Egan *et al.*, 1957). The association of the molecules is also dependent upon the ionic strength or salt concentration of the aqueous solution (Aune *et al.*, 1971), all of which implicates ionic groups in the association interactions. Photooxidation of a single histidine residue in α-chymotrypsin causes the disappearance of any tendency for α-chymotrypsin to associate and this led to the idea that a charged imidazole and a carboxylate ion were involved in an association interaction (Egan *et al.*, 1957). In a similar way, Tyr-146 has been implicated in the dimerization interaction by the fact that its removal from the B-chain terminus with carboxypeptidase yields a product incapable of forming dimers (Gladner and Neurath, 1954). The foregoing led Aune and Timasheff (1971) to analyze the dimerization equilibrium constants as a function of pH. After some assumptions concerning the system (no conformational changes with pH, no group pK changes with dimerization), they fitted the observed pH dependence of the dimerization equilibrium constant by calculating the pH dependence of the free energy of electrostatic interaction between monomeric molecules in terms of pK values of ionic groups on the enzyme. The results indicated that two ionic groups shift their pK values during dimerization: one from pK 5.0 (monomer) to 6.2 (dimer) and the other from pK 3.6 (monomer) to 2.4 (dimer). Utilizing the reciprocity in the calculated behavior, the most likely groups to be involved in the observed pH range and the structure of α-chymotrypsin based on that of inhibited tosyl-α-chymotrypsin (Birktoft *et al.*, 1969), Aune and Timasheff (1971) proposed that the observed pH dependence of the dimerization could essentially be accounted for by an interaction of the imidazolium ion of His-57 with a terminal carboxylate ion of Tyr′-146. Other known interface ionic interactions were discounted or said to serve only to increase the free energy of formation of the dimer and not to affect the pH dependence of the process.

Since our results of the dimeric structure of native α-chymotrypsin at pH 4.2 indicate a close approach to the α-carboxylic acid group of Tyr′-146 to His-57 (4.5–5.0 Å to the center of the imidazolium ring), the foregoing imidazolium–carboxylate interaction is consistent with the structure. However, upon further consideration, a number of difficulties become apparent. Although the imidazole of His-57 is certainly protonated at pH 4.2, the ionization state of the carboxylic acid group of Tyr-146 *in the dimeric structure* is somewhat uncertain. For one thing, it is buried within the molecule of the dimer so that its pK might be higher than that ordinarily expected of a terminal carboxyl group. Furthermore, at pH 4.2, one of the carboxylate oxygen atoms (O_2) of the Tyr′-146 comes within about 3.0 Å of the oxygen of the carbonyl of His-57; this suggests that a hydrogen bond is formed between these two atoms and that the carboxyl group is protonated (Figure 3). The positive charge of the imidazolium ion at pH 4.2 in the dimeric structure is satisfied by the charge of Asp-102 (Blow *et al.*, 1969) and the hydrogen-bonded bridging sulfate ion (about 4.5 Å from the imidazolium ion) which is located between O_γ of Ser-195 and the hydroxyl group of Tyr′-146; the sulfate ion is additionally accompanied by a peak about 4.0 Å away which has tentatively been assigned to correspond to a cation (H_3O^+ or NH_4^+), thus neutralizing some of the charge of the sulfate ion (Figure 3).

Upon change of pH to 6.7, the most significant change that occurs in this region of the dimer is that associated with the terminal carboxyl group of Tyr′-146; only a minor movement is observed with the imidazolium ion of His-57. Although the imidazolium ion might lose its proton at this pH and a carboxylate group of Tyr′-146 might consequently move to a more favorable environment, the observed significant movement resides solely in the carboxylate of Tyr′-146. Furthermore, the movement is such that the closeness of the original contacts between His-57 and Tyr-146 is maintained suggesting that an original interaction is disrupted but that an interaction remains, possibly of a different kind. Considering that His-40 undergoes a large orientational change at pH 6.7, it would seem that His-57 might not in fact be deprotonated at this pH in the dimeric structure and that it might have a somewhat higher pK than this value. Such a notion is further supported by the fact that the bridging sulfate ion remains unaffected by the change in pH probably still interacting with the imidazolium charge. Thus, an equally likely occurrence consistent with the observations is that the carboxylic acid group of Tyr′-146 with a higher pK than usual ionizes to a carboxylate ion at pH 6.7. The original hydrogen bond to the His-57 carbonyl at pH 4.2 is disrupted and the carboxylate ion enters into an ionic interaction with the imidazolium ion at pH 6.7. The true situation might be discerned from the results of our work at pH 8.6, where the His-57 is surely deprotonated.

It is quite possible that the movements observed in the Phe-39 and the Ser-217–Ser-218 regions of the interface are not directly related to the change in pH of the surrounding medium. When the dimeric molecule is formed, strong ionic and other electrostatic interactions elsewhere force one or the other or both residues of these pairs to adopt strained configurations in order to accommodate one another (Tulinsky *et al.*, 1973b). When the pH is increased, the groups responsible for the interface interactions tend to separate within their confined crystalline matrix because of the disruption of strong interactions so that the forementioned residues might simply be moving to relieve or adjust the original strain. The Met-192–Met′-192 interaction also falls into this category. The C_γ of Met-192 rotates in a clockwise manner about the C_β–C_γ bond relieving a very close van der Waals contact by moving the sulfur atom away from the local twofold axis. The twofold related Met′-192 shows no changes. Finally, it should be noted that in the case of the latter two crowded situations (Ser-217–Ser-218, Met-192), it is the region closer to the local twofold axis which shows the larger and most number of changes.

His-40. Since histidine residues typically have a pK of about 6.5, the imidazole ring of His-40 must be protonated and positively charged at pH 4.2. The charge is apparently neutralized by the presence of the carboxylate ion of Asp-72 which is located nearby about 4.5 Å away. Upon change in pH to 6.7, the His-40 shows a fairly large reorientation of its imidazole ring. The movement of the imidazole could be associated with a change in interaction upon deprotonation. This agrees well with the observed fluorescence behavior of δ-chymotrypsin as a function of pH (Hess *et al.*, 1970). The fluorescence of δ-chymotrypsin decreases with decreasing pH as an ionizing group of pK ≃6.0 apparently gains a proton. Model studies have shown that the fluorescence of tryptophan is quenched when a complex is formed between the indole ring of tryptophan through a charge-transfer interaction with a protonated imidazole (about −3 kcal/mol stabilization energy) (Shintzky *et al.*, 1966; Shintzky and Goldman, 1967). An increase in fluorescence occurs when the imidazole ionizes and the complex is disrupted. The proximity of His-40 and Trp-141 in the structure of α-chymotrypsin has already been mentioned so that these two residues probably interact at lower pH values to form such a charge-transfer complex. The ionization of His-40 at higher pH and its subsequent movement destroy the complex which then leads to the observed increase in tryptophan fluorescence.

Uranyl Binding Region. The proximity of Glu-21 and Asp′-153 in crystals of α-chymotrypsin at pH 4.2 suggests that hydrogen bonding or possibly a specific site–site interaction due to fluctuation in charge configuration might be occurring in this intermolecular region (Kirkwood and Shumaker, 1952a,b; Timasheff, 1966). Such an interaction results when a proton fluctuates between two ionizable groups with similar free energies of ionization. Moreover, the effect is at its optimal in the pH region of the pK values of the ionizable groups and is accompanied by a stabilization energy of 1–2 kcal/mol. Since the pK values of Asp and Glu acids have been reported to be 4.1 and 4.5, respectively (Nozaki and Tanford, 1967), it would seem that the proton–charge interaction would be near its maximum in the native structure of the enzyme (pH 4.2). Upon raising the pH to 6.7, one or both protons would be lost and the interaction would be destroyed. This would then probably lead to a repositioning of these residues as observed in the pH difference map to favorably accommodate the increase in charge in the region. It is also consistent with the observed rearrangements of the guanidinium ion of Arg-154 and a localized sulfate ion in this region. It also implies that either Glu-21 or Asp′-153 or both are protonated at pH 4.2. However, all the foregoing can also be practically accounted for in terms of hydrogen bonding between adjacent carboxylic acid groups.

Acknowledgment

We would like to thank Mr. Michael N. Liebman for useful discussions and comments concerning this work.

References

Aune, K. C., Goldsmith, L. C., and Timasheff, S. N. (1971), *Biochemistry 10*, 1617.

Aune, K. C., and Timasheff, S. N. (1971), *Biochemistry 10*, 1609.

Bender, M. L., Clement, G. E., Kezdy, F. J., and d'A Heck, H. (1964), *J. Amer. Chem. Soc. 86*, 3680.

Bender, M. L., and Kezdy, F. J. (1965), *Annu. Rev. Biochem. 34*, 49.

Birktoft, J. J., and Blow, D. M. (1972), *J. Mol. Biol. 68*, 187.

Birktoft, J. J., Matthews, B. W., and Blow, D. M. (1969), *Biochem. Biophys. Res. Commun., 36*, 131.

Blow, D. M., Birktoft, J. J., and Hartley, B. S. (1969), *Nature (London) 221*, 337.

Blow, D. M., and Crick, F. H. C. (1959), *Acta Crystallogr. 12*, 794.

Blow, D. M., Rossmann, M. G., and Jeffery, B. A. (1964), *J. Mol. Biol. 8*, 65.

Cohen, G. H., Matthews, B. W., and Davies, D. R. (1970), *Acta Crystallogr., Sect. B 26*, 1062.

Doscher, M. S., and Richards, F. M. (1963), *J. Biol. Chem. 238*, 2399.

Egan, R., Michael, H. O., Schlueter, R., and Jandorf, B. J. (1957), *Arch. Biochem. Biophys. Acta 94*, 535.

Gladner, J. A., and Neurath, H. (1954), *J. Biol. Chem. 206*, 911.

Henderson, R., and Moffat, J. K. (1971), *Acta Crystallogr., Sect. B 27*, 1414.

Hess, G. P. (1971), *Enzymes, 3rd Ed., 3*, 213.

Hess, G. P., McConn, J., Ku, E., and McConkey, G. (1970), *Phil. Trans. Roy. Soc. London, Ser. B 257*, 89.

Kirkwood, J. G., and Shumaker, J. B. (1952a), *Proc. Nat. Acad. Sci. U. S., 38*, 855.

Kirkwood, J. G., and Shumaker, J. B. (1952b), *Proc. Nat. Acad. Sci. U. S. 38*, 863.

Lumry, R., and Biltonen, R. (1969), *in* Structure and Stability of Biological Molecules, Timasheff, S. N., and Fasman, G. D., Ed., New York, N. Y., Marcel Dekker, p 65.

Luzzatti, V. (1953), *Acta Crystallogr. 6*, 142.

Matthews, B. W., Sigler, P. B., Henderson, R., and Blow, D. M. (1967), *Nature (London), 214*, 652.

Nozaki, V., and Tanford, C. (1967), *J. Biol. Chem. 242*, 4731.

Quiocho, F. A., and Richards, F. M. (1966), *Biochemistry 5*, 4062.

Richards, F. M. (1968), *J. Mol. Biol. 37*, 225.

Rossi, G. L., and Bernhard, S. A. (1970), *J. Mol. Biol. 49*, 85.

Schwert, G. W. (1949), *J. Biol. Chem. 179*, 655.

Schwert, G. W., and Kaufman, S. (1951), *J. Biol. Chem. 190*, 807.

Shintzky, M., and Goldman, R. (1967), *Eur. J. Biochem. 3*,

139.
Shintzky, M., Katchalski, E., Grisaro, V., and Sharon, N. (1966), *Arch. Biochem. Biophys. 116*, 332.
Timasheff, S. N. (1966), *Biopolymers 4*, 107.
Tulinsky, A., Mani, N. V., Morimoto, C. N. and Vandlen, R. L. (1973a), *Acta Crystallogr., Sect. B. 29*, 1309.
Tulinsky, A., Vandlen, R. L., Morimoto, C. N., Mani, N. V. and Wright, L. H. (1973b), *Biochemistry 12*, 4185.
Tulinsky, A., and Wright, L. H. (1973), *J. Mol. Biol.* (in press).
Vandlen, R. L., and Tulinsky, A. (1971a), 67th Annual Meeting of the American Society of Biological Chemists, San Francisco, Calif., June, No. 444.
Vandlen, R. L., and Tulinsky, A. (1971b), *Acta Crystallogr., Sect. B 27*, 437.

Flavine–Protein Interactions in Flavoenzymes. pH Dependence of the Binding of Flavine Mononucleotide and Riboflavine to *Azotobacter* Flavodoxin†

Martha L. MacKnight, James M. Gillard, and Gordon Tollin*

ABSTRACT: In order to specify the ionization state of the ribityl phosphate group in the bound flavine mononucleotide (FMN), and also to determine whether any ionizable protein side-chain groups are involved directly or indirectly in flavine binding, we have studied the pH dependence of the interaction between *Azotobacter* apoflavodoxin and FMN and riboflavine. Both kinetics and equilibria have been investigated. Below pH 3.5, FMN is reversibly released from the holoprotein. This follows a two-proton dependence with a pK of 3 (suggestive of protein side-chain carboxyls). Circular dichroism (CD) spectra demonstrate a change in protein conformation accompanying this release. The second-order rate constants for FMN binding to the apoprotein increase by approximately a factor of 40 between pH 8 and 3.7. Riboflavine shows a much smaller increase in this region. At least two pK values are required to fit the FMN data. The equilibrium constants for both FMN and riboflavine binding do not change appreciably between pH 8 and pH 5. Below pH 5, both analogs show a decrease in binding. FMN follows a curve with a midpoint of about 3.5. Riboflavine displays a more complex behavior involving a rapid fluorescence decrease followed by a slower increase; the latter corresponds to a pK of about 4.5. These results are interpreted as follows. FMN can bind to the apoprotein as both the dianion and the monoanion (referring to the phosphate group). The dianion is released from the protein about 10 times more slowly than is the monoanion. This raises the possibility that positively charged protein side-chain groups are involved in an interaction with the negatively charged phosphate group. Two protein side-chain carboxyls are required to be in their negatively charged forms in order for effective binding to occur. The pK of these carboxyls is ~4 in the apoprotein and is shifted to about 3 in the holoprotein.

Interest in the flavodoxins has been heightened by the recent publication of medium resolution X-ray structures (Watenpaugh *et al.*, 1972; Andersen *et al.*, 1972) for two of these proteins which show the polypeptide chain folding pattern and the orientation of the FMN molecule in the binding site. Although all of the protein side-chain groups which interact with the flavine have not yet been identified, among the features which are clearly specified are the following: (a) the phosphate binding site is located very near to the N terminus of the protein; (b) the entire ribityl phosphate side chain is largely buried within the protein. The latter point is consistent with a variety of kinetic and thermodynamic measurements of flavine binding to several apoflavodoxins (Edmondson and Tollin, 1971c; Barman and Tollin, 1972a). Furthermore, a high degree of homology has been found to exist in the N-terminal region of four of these proteins, specifically those obtained from *Peptostreptococcus elsdenii* (Tanaka *et al.*, 1971), *Desulfovibrio vulgaris* (Dubourdieu *et al.*, 1973), *Clostridium pasteurianum* (Fox *et al.*, 1972; J. L. Fox, personal communication), and *Azotobacter vinelandii* (M. L. MacKnight, W. L. Gray, and G. Tollin, manuscript in preparation).

In order to specify the ionization state of the ribityl phosphate group in the bound cofactor, and also to determine whether any ionizable protein side-chain groups are involved directly or indirectly in flavine binding, we have studied the pH dependence of the interaction between *Azotobacter* apoflavodoxin and FMN and riboflavine. This flavodoxin is of particular interest because of its highly stable free-radical form (Hinkson and Bulen, 1967; Edmondson and Tollin, 1971c), its function as the electron donor to nitrogenase in nitrogen fixation (Yates, 1972), and its unusually high first reduction potential (Barman and Tollin, 1972b). Three previous investigations of the effect of pH on flavine binding to a flavoprotein have been reported, *P. elsdenii* flavodoxin (Mayhew, 1971a), *Azotobacter* flavodoxin (Hinkson, 1968), and old yellow enzyme (Theorell and Nygaard, 1954). Only in the case of the old yellow enzyme was the study extensive enough to establish the ionization state of the FMN phosphate on the protein and to provide evidence for the involvement of ionizable protein functional groups in binding.

† From the Department of Chemistry, University of Arizona, Tucson, Arizona 85721. *Received June 5, 1973.* This work was supported in part by a grant from the National Institutes of Health (1R01-AM15057). Presented in part at the Flavins and Flavoproteins International Workshop, Konstanz, Germany, March, 1972.